Wind and Structures, Vol. 12, No. 2 (2009) 89-101
DOI: http://dx.doi.org/10.12989/was.2009.12.2.089

Analysis of light-frame, low-rise buildings under simulated lateral wind loads

C. Fischer

Institute of Theoretical and Applied Mechanics, Academy of Sciences, Prosecka 76, 190 00 Prague 9, Czech Republic

B. Kasal*

Department of Civil and Environmental Engineering; Department of Architectural Engineering, Penn State University, University Park, PA 16802, USA

(Received October 11, 2007, Accepted December 18, 2008)

Abstract. The Monte Carlo procedure was used to simulate wind load effects on a light-frame low-rise structure of irregular shape and a main wind force resisting system. Two analytical models were studied: rigid-beam and rigid-plate models. The models assumed that roof diaphragms were rigid beam or rigid plate and shear walls controlled system behavior and failure. The parameters defining wall stiffness, including imperfections, were random and included wall stiffness, wall capacity and yield displacements. The effect of openings was included in the simulation via a set of discrete multipliers with uniform distribution. One and two-story buildings were analyzed and the models can be expanded into multiple-floor structures provided that the assumptions made in this paper are not violated.

Keywords: low-rise building; simplified models; wind loads; stochastic analysis.

1. Introduction

In the United States, over 95% of all residential structures are designed as light-frame buildings. The majority of these types of structures is designed as low-rise buildings with a maximum of two stories. Wood-stud frame systems are used in over 90% of the designs. Due to their low masses, the light-frame buildings (LFB) perform well under a short-term dynamic load such as an earthquake but are vulnerable in high winds where significant structural damage is a concern, mainly in hurricane-prone regions. Strong winds can be destructive for LFBs, due to their low masses and limited resistance to negative pressure components. After Hurricane Andrew (Cook and Soltani 1994), national codes in the US reflected on lessons learned and adopted guidelines governing the construction of LFBs and prescriptive bracing requirements (IRC 2006). Bracing requirements are geared toward providing lateral resistance of the entire structure, are based on shear wall performance and the lowest bracing requirements cover areas with wind speeds at or below 44.7 m/s

* Professor, Corresponding Author, E-mail: Bo_Kasal@engr.psu.edu

(100 mph) and seismic categories defined as A and B (IRC 2006). This requirement may have an adverse impact on residential structures located in areas with lower-than 44.7 m/s wind speeds and low seismicity. While the building code requirements are a positive step to ensuring safety, the nature of these prescriptive requirements is not entirely clear; the requirements are based on a tributary area approach, simple rectangular building shapes and a deterministic analysis - see Kasal and Crandell (2007).

Laboratory experiments have shown that analytical modeling of wind-induced, structural response of LFBs is possible (Kasal, *et al.* 1999, and Pavere, *et al.* 2003). The deterministic models showed acceptable predictive power and reasonable estimates of load paths (Kasal, *et al.* 1999, Pavere, *et al.* 2003, Collins, *et al.* 2005a,b). An approach to combining stochastic and deterministic analyses had been proposed, but no sufficient experimental data existed to explore the applicability of it to the analysis and design of LFBs (IRC 2006).

The wind loads on low-rise buildings have been simulated using mostly wind tunnel experiments; little information is available from in-situ full-scale tests. Data from instrumented full-scale LFBs tested in Canada will permit further verification of deterministic models and will allow for the validation of scaled wind tunnel experiments, as it is shown in Smith and Kasal (2004). Recently, database-assisted design (DAD) has been proposed by Whalen, *et al.* (1998a,b), in which time histories of pressures that are measured at a large number of points on the structure envelope are used to simulate the response of a structure over a given period of time - see Sadek, *et al.* (2004). The known problem with low-rise structures is that the spatial pressure distribution is affected by the surrounding terrain and the building response is non-Gaussian, as indicated by Sadek and Simiu (2002). The authors report that using one hour sample records to estimate the peak responses has high variability and propose using the entire data sets contained in the time series. They used a probability plot correlation coefficient (PPCC) method and proposed Extreme Value Type I (Gumbel), Reverse Weibull and Gamma distributions to model the largest response peaks. The aerodynamic databases, as reported e.g. by Whalen, *et al.* (1998b) were successfully applied to main wind force resisting systems (MWFRS) (portal frames) analysis. The most recent work by Hanzlík, *et al.* (2005) shows that building orientation and wind effects can be successfully modeled with the DAD approach. Corotis and Dougherty (2004) studied wind records from 5 different locations and used 6 different types of distributions and the peak-over-thresholds approach to calculate the expected wind speeds for different return periods. They concluded that the calibrated probability distributions, even if filtered, were unreliable even for short return periods.

Rosowski and Cheng (1999a, b) studied the reliability of roof systems in high-wind regions. They used the Extreme Value Type I distribution to describe wind speed and the ASCE 7-95 (2005) and 7-93 standards and a tributary area approach for spatial pressure distribution. Properties of panel-to-frame connections were random. Although the analytical model that was used in this study has not been described, the work represents an interesting insight into roof performance, even if the load sharing and redistribution has not been fully accounted for. Pinelli, *et al.* (2004) presented a probabilistic framework for annual damage estimation resulting from windstorms using the Monte Carlo simulation that related probabilistic loads and resistances. Five basic damage modes were defined that included roof sheathing and roof-to-wall connections. The structural engineering analysis and Monte Carlo simulations were identified as critical issues. The structural models were identified as one of the key components of uncertainties.

2. Simplified analytical models

Analytical models are frequently used to simulate the expected behavior of a system and can have different varying degrees of complexity. More complex and computationally demanding models, presented e.g. by Collins, *et al.* (2005a, b) or Kasal, *et al.* (2004) yield more accurate results but are not particularly suitable for stochastic analyses where computational efficiency is critical. The common feature of complex models is that they are relatively inefficient, slowly converging and relatively difficult to develop, due to their complex geometries. Complex numerical models are, in most cases, not suitable for stochastic analyses since no closed-form solutions exist. However, complex models can yield information about local behavior and failure modes. Such level of accuracy is usually lost in simplified models. Simplified analytical models are needed to obtain a reasonable estimate of statistics needed to describe failure probability. Model accuracy and correct load representation constitute two fundamental problems in the simulation procedures.

The model must be computationally efficient to permit repeated analyses. This generally requires significant simplifications of the complex geometries, material and connection properties. Such simplifications may result in a loss of predictive power of the physical behavior. The accuracy of various simplified analytical models of LFBs has been discussed in the work of Kasal, *et al.* (2004) and compared with the full-scale experiments. A loss of information resulting from model simplification was demonstrated and quantified.

The LFB can be represented as a system of horizontal diaphragms and vertical shear walls. The horizontal diaphragms distribute forces into shear walls which then transfer them to the foundation. This simplified approach to analyze LFBs subjected to lateral loads has been used in analyses of such structures subjected to wind loads and assumes that the shear walls are a key component controlling the safety of the LFB under lateral loads. This is true when one studies the main wind force resisting system (MWFRS), and not local wind effects on a building (components and cladding).

The focus of this paper is to show how MWFRS and two relatively simple analytical models are used to represent the LFB: rigid-beam and rigid-plate models. The performance of both of these models is demonstrated on the existing LFB structure described in Collins, *et al.* (2005a, b), Foliente, *et al.* (2000), Kasal, *et al.* (2004) and shown in Fig. 1. In both models, the diaphragm is assumed to be rigid and no slip between the walls and the diaphragm is permitted. The walls are represented as linear or nonlinear springs.

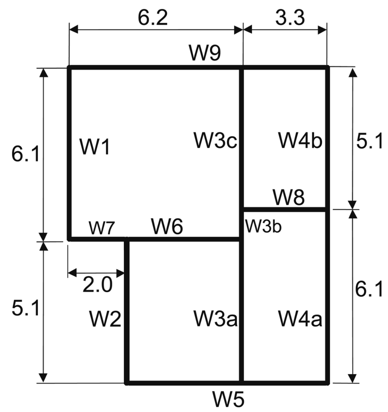

Fig. 1 Floor plan of the tested structure (dimensions in m).

2.1. The rigid beam model

In this model, the diaphragm of each floor is represented by a rigid beam supported by uni-directional springs representing shear walls. Only the walls perpendicular to the beam orientation are accounted for as lateral resisting elements – see Fig. 2a. The model is one-dimensional and will thus overestimate the building's response to a lateral load. The location of individual walls is determined by the variable x_i for $i = 1.. \; m_{y,s}$, where $m_{y,s}$ is number of walls of floor s oriented in the y direction. The deformation in the point (wall) $x_{s,i}$ is designated as $\Delta_{s,i}$. The geometrical condition of rigidity (see equations below for the rigid plate) is written as

$$\Delta_{s,i} = \lambda_s x_i + \gamma_s \tag{1}$$

The parameters λ_s and γ_s represent the rotation and translation of the beam representing floor s. Two conditions for force and moment equilibrium for each diaphragm are available:

$$\sum_{i=1}^{m_{y,s}} k_{y,s,i}(\Delta_{s,i} - \Delta_{s-1,i}) - F_{y,s} - \sum_{j=1}^{m_{y,s+1}} F_{y,s+1,j} = 0, \quad \Delta_{0,i} = 0 \tag{2}$$

$$\sum_{i=1}^{m_{y,s}} k_{y,s,i}(\Delta_{s,i} - \Delta_{s-1,i})x_{s,i} - F_{y,s}\rho_{y,s} - \sum_{j=1}^{m_{y,s+1}} F_{y,s+1,j}\rho_{y,s+1,j} = 0 \tag{3}$$

where $k_{y,s,i}(\Delta_{s,i})$ is the corresponding nonlinear stiffness of wall i (or nonlinear spring, i) as a function of the displacement $\Delta_{s,i}$ at the point $x_{s,i}$; $F_{y,s}$ is the resultant force from the wind pressure acting at level s, and at location $\rho_{y,s}$; $F_{y,s+1,j}$ is the reaction force from the floor above in wall j at the location of $\rho_{y,s+1;}$ and $m_{y,s+1}$ is the number of walls in the floor above.

The reaction forces $F_{y,s+1,j}$ can be expressed in terms of displacements $\Delta_{s+1,i}$, which permits us to write Eqs. (2)-(3) in the form:

$$\begin{gathered}\sum_{i=1}^{m_{y,s}} k_{y,s,i}(\Delta_{s,i} - \Delta_{s-1,i}) - \sum_{j=1}^{m_{y,s+1}} K_{y,s+1,i}(\Delta_{s+1,i} - \Delta_{s,i}) - F_{y,s} = 0 \\ \sum_{i=1}^{m_{y,s}} k_{y,s,i}(\Delta_{s,i} - \Delta_{s-1,i})x_{s,i} - \sum_{j=1}^{m_{y,s+1}} K_{y,s+1,i}(\Delta_{s+1,i} - \Delta_{s,i})x_{s+1,i} - F_{y,s}\rho_{y,s} = 0\end{gathered} \tag{4}$$

For a single story and the top floor of a multi-story building, the $F_{y,s+1}$ terms in Eqs. (2)-(3) and the values of $m_{y,s+1}$, $\Delta_{s+1,i}$, $x_{y,s+1}$ in Eq. (4) will be zero.

Using the pressure resultant to represent the wind pressures is convenient, since the pressure distribution function may not be known and is, by itself, a random variable. $F_{y,s}$ can be calculated as

$$F_{y,s} = \int_A p(x, z_s)\,dA \tag{5}$$

where $p(x,z)$ is the pressure distribution function defined over the area $A(x,z)$ (normal to the direction of force $F_{y,s}$), and z is the coordinate along the height of the building corresponding to floor s. The location of the resultant force $F_{y,s}$ can be calculated as

$$\rho_{y,s} = \frac{\int_A x p(x, z_s) dA}{\int_A p(x, z_s) dA} \tag{6}$$

where x is the coordinate along the length of the beam.

2.2. The rigid plate model

Each floor of the building is substituted by a rigid plate. Each plate is allowed to shift and rotate within its plane and the model captures the translation and rotation of the building. A set of n points with coordinates (x_i ,y_i) is used to define the plate geometry, with each point corresponding with the center of each wall. For the sake of simplicity, the geometry of each floor is assumed to be constant. Because the model is two-dimensional, the effect of transverse walls on the building's response is accounted for. Although the model can be expanded to include the bending stiffness of the walls, the bending stiffness was considered negligible compared to the in-plane wall stiffness and was neglected in subsequent analyses. If known (for example from a detailed analysis or experiments), the bending stiffness can be lumped into the shear wall stiffness.

Individual walls can either be represented by a single spring along the x- or y-axes or divided into subsections with each subsection represented by a separate spring – see Fig. 2b. The model permits the inclusion of interior walls as bracing elements. Such contribution to the building's overall stiffness is frequently neglected.

Assuming a rigid plate, a general expression for the displacement of point (x_i ,y_i) of floor s can be written as:

$$\begin{pmatrix} \delta x_{s,i} \\ \delta y_{s,i} \end{pmatrix} = \begin{pmatrix} \xi_s + x_i(\cos\phi_s - 1) - y_i \sin\phi_s \\ \eta_s + x_i \sin\phi_s + y_i(\cos\phi_s - 1) \end{pmatrix} \approx \begin{pmatrix} \xi_s - y_i\phi_s \\ \eta_s + x_i\phi_s \end{pmatrix} \tag{7}$$

where ξ_s, η_s and ϕ_s describe the rigid body translations and rotations of the diaphragm s; $\delta x_{s,i}$, $\delta y_{s,i}$

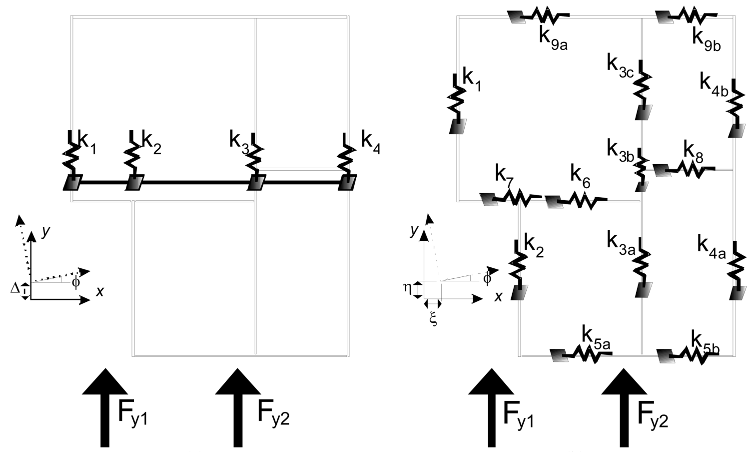

(a) (b)

Fig. 2 Schematic of the beam model (a) and the plate model (b) are deformations of point i at level s in the directions of x and y; $k_{x,s,i}(\delta x_{s,i})$ and $k_{y,s,i}(\delta y_{s,i})$ and are the corresponding stiffnesses. Since the rotation angle ϕ_s is small, the usual simplification in Eq. (7) can be used resulting in the right-hand side without trigonometric functions.

The equilibrium of forces in the x and y directions and a moment condition are used to obtain the three unknowns ξ_s, η_s and ϕ_s for each floor:

Using the force equilibrium:

$$\sum_{i=1}^{m} k_{x,s,i}(\delta x_{s,i} - \delta x_{s-1,i}) - F_{x,s} - \sum_{j=1}^{m} F_{x,s+1,j} = 0 \tag{8}$$

$$\sum_{i=1}^{m} k_{y,s,i}(\delta y_{s,i} - \delta y_{s-1,i}) - F_{y,s} - \sum_{j=1}^{m} F_{y,s+1,j} = 0 \tag{9}$$

where $F_{x,s}$ and $F_{y,s}$ are the external forces acting on the system in the x and y directions corresponding to floor s, $F_{x,s+1,j}$ and $F_{y,s+1,j}$ are reaction forces from the walls above; and m is the number of walls (m is common for each floor).

Using the moment condition with respect to the center $(0, 0)$:

$$\sum_{i=1}^{m} k_{x,s,i}(\delta x_{s,i} - \delta x_{s-1,i})y_i - \sum_{i=1}^{m} k_{y,s,i}(\delta y_{s,i} - \delta y_{s-1,i})x_i - F_{x,s}\rho_{x,s} + F_{y,s}\rho_{y,s} + \sum_{j=1}^{m} x_j F_{y,s,j} - \sum_{j=1}^{m} y_j F_{x,s,j} = 0 \tag{10}$$

where $\rho_{x,s}$ and $\rho_{y,s}$ are the x and y coordinates of the point where the forces $F_{x,s}$ and $F_{y,s}$ are acting on floor s.

If the reaction forces are expressed using the displacements of the floor above, the Eqs. (8)-(10) simplify into the form

$$\begin{aligned}
&\sum_{i=1}^{m} k_{x,s,i}(\delta x_{s,i} - \delta x_{s-1,i}) - \sum_{j=1}^{m} k_{x,s+1,i}(\delta x_{s+1,i} - \delta x_{s,i}) - F_{x,s} = 0 \\
&\sum_{i=1}^{m} k_{y,s,i}(\delta y_{s,i} - \delta y_{s-1,i}) - \sum_{j=1}^{m} k_{y,s+1,i}(\delta y_{s+1,i} - \delta y_{s,i}) - F_{y,s} = 0 \\
&\sum_{i=1}^{m} (k_{x,s,i}(\delta x_{s,i} - \delta x_{s-1,i}) - k_{x,s+1,i}(\delta x_{s+1,i} - \delta x_{s,i}))y_i - \\
&\sum_{i=1}^{m} (k_{y,s,i}(\delta y_{s,i} - \delta y_{s-1,i}) - k_{y,s+1,i}(\delta y_{s+1,i} - \delta y_{s,i}))x_i - F_{x,s}\rho_{x,s} + F_{y,s}\rho_{y,s} = 0
\end{aligned} \tag{11}$$

Setting $\delta x_{N+1,i} = \delta x_{N,i}$, $\delta y_{N+1,i} = \delta y_{N,i}$, $\delta x_{0,i} = 0$ and $\delta y_{0,i} = 0$ ensures that Eq. (11) is valid for the last floor N.

For the linear springs, Eq. (11) can be linearized using the assumption of small rotation ϕ_s – Eq. (7).

In this paper only a uni-directional load (wind pressure along the y direction) was used but the plate model can be also used for bi-directional loading (x- and y- directions simultaneously). The single direction is used for the purpose of comparison of the beam and plate models. The resultant force $F_{X,s}$ and its location $\rho_{x,s}$ can be calculated using Eqs. (5) and (6) by integrating over the plane x-z.

2.4. Shear walls

A piecewise linear function was used to represent the load-deformation characteristic of the shear walls due to its simplicity but any type of function, such as polynomial or exponential functions, can be used. Parameters defining the function can be obtained either from experiments or analytical models. To model the uncertainty of the generic stiffness function, the actual measured stiffness was scaled by two normally distributed random variables χ_1, χ_2 with mean 1.0 and variance 0.1 in the following way:

$$k(\delta) = \chi_1 k_0(\chi_2 \delta) \tag{12}$$

where $k_0(\delta)$ is the generic stiffness function. Hence, the stiffness function varies within 20% - see Fig. 3.

A convenient method to simulate different wall stiffnesses is to use a generic stiffness function $k(\delta)$ and a set of multipliers that can be used to change the generic function to represent different load-deformation curves.

The stiffness of a single wall within floor s for a particular run is:

$$\begin{aligned} k_{x,s,i}(\delta) &= k_{x,s,type} k_{x,s,w} k_{x,s,i} \chi_1 k_0(\chi_2 \delta) \\ k_{y,s,i}(\delta) &= k_{y,s,type} k_{y,s,w} k_{y,s,i} \chi_1 k_0(\chi_2 \delta) \end{aligned} \tag{13}$$

where

$k_0(\chi_2\delta)$ is the generic stiffness function,

$k_{x,s,i}$ and $k_{y,s,i}$ are the deterministic multipliers to model the stiffness of the particular wall in the x or y direction on level s,

$k_{x,s,w}$ and $k_{y,s,w}$ are normal, random variables with mean 1 and variance 0.15 modeling the variability of the structure of the wall. The value of the variance reflects the uncertainty in wall construction practice.

$k_{x,s,type}$ and $k_{y,s,type}$ are uniformly distributed, random coefficients taking the values of 0.3, 0.6, 0.8 and 1.0 and simulating openings in the individual walls,

χ_1, χ_2 are normal, random variables with mean 1.0 and variance 0.1 describing the uncertainty of the generic stiffness function. The value of the variance is based on shear wall tests of identical construction, performed by Memari, *et al.* (2008), that indicate a relatively low variability of stiffness and capacity between shear walls of the same construction.

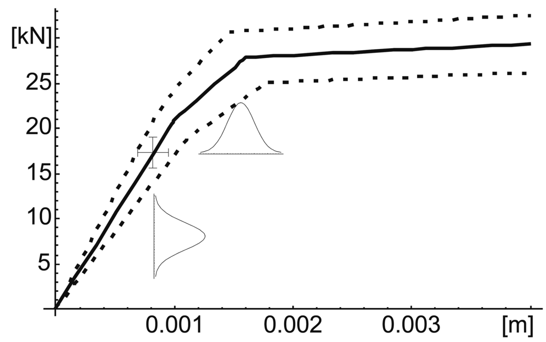

Fig. 3 Example of the load-deformation curve of the shear wall

The multipliers change the shape of the stiffness function and reflect the potential variable stiffness of individual walls. Moreover, individual walls are characterized by an additional uniformly distributed coefficient representing various openings in the wall.

The generic stiffness functions of the walls, $k_0(\delta)$, were based on experimental results reported by Collins, *et al.* (2005a,b), Foliente, *et al.* (2000) and Kasal, *et al.* (2004). The multipliers $k_{x,s,type}$ and $k_{y,s,type}$ represent a reasonable assumption of the reduction of wall stiffness due to the presence of openings. These values will be fixed for a known design or for code studies where the amount of bracing is prescribed as a percentage of the braced wall line length, see IRC (2006). Note the spacing between the first two multipliers representing wall opening (0.3 and 0.6) that will result in a bi-modal distribution if the spacing is larger than the variances of the other multipliers. The multipliers defined above represent a convenient mathematical formulation where a single generic stiffness function can be used for all walls and its shape can be varied. One can use a set of functions to describe the stiffness of each shear wall and limit the multipliers to only model uncertainties in wall stiffness and/or the presence of openings.

2.5. Wind loading

A known expression reported by Simiu and Scanlan (1996) was used to calculate wind force and only the y-direction was considered:

$$F = Ac\frac{1}{2}\rho_a v^2 \tag{14}$$

where v is the wind speed, ρ_a is the air density in consistent units, and A is the area over which the wind is acting. The Reverse Weilbull distribution, described by its cumulative density function $P_v(v)$ and distribution function $P_v(v)$ was used to represent the wind speed in m/s - see e.g. Grigoriu (2006)

$$P_v(v) = \exp\left\{-\left(\frac{-\zeta-v}{\alpha}\right)^{\theta}\right\}, \quad p_v(v) = \frac{\theta}{\alpha}\left(\frac{-\zeta-v}{\alpha}\right)^{\theta-1}\exp\left\{-\left(\frac{-\zeta-v}{\alpha}\right)^{\theta}\right\} \tag{15}$$

with parameters $\alpha = 42.6684$, $\theta = 11.3373$ and $\zeta = -50.7514$ (see Fig. 4).

These values were obtained from yearly maxima of the peak gust wind speed (m/s) measured at Pueblo, CO, USA. The wind-speed data set available at the National Institute of Standards (NIST) database was used (Extreme Wind Speed Data Sets). In this study, we used uniformly distributed wind pressure but any reasonable function describing wind pressure spatial distribution (over the building length) can be used.

3. Numerical results

The generic stiffness function $k_0(\delta)$ described above can be approximated by a piecewise linear function. Its shape originates from experiments published by Paevere, *et al.* (2003). These experiments showed that at the corresponding design wind load, the tested structure displaced about 1-2 mm laterally. Previous testing of individual walls showed that at a relative displacement of about 1%, the overall stiffness decreases and a yielding effect occurs. Thus, the occurrence of such a loss of stiffness was used as a failure criterion.

The bearing capacity of the individual wall is consequently defined as the force causing non-linear

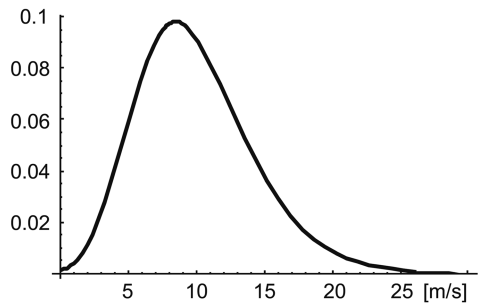

Fig. 4 Wind speed distribution governed by the Eq. (11)

behavior of the stiffness function. Failure occurs when the reaction of a wall exceeds its bearing capacity.

In the first example, the geometric parameters of the structure were held fixed. This means that the position and size of the openings were not varied in the walls and the only random variable was the wall stiffness itself. The loading force followed the probability distribution according to Eq. (15) and the wall stiffness followed the normal distribution (with a variability of 20 %) around the nominal stiffness obtained from the experiments (Foliente, *et al.* 2000). The bearing capacity of individual walls depends on the shape of the general stiffness function, namely on the variable χ_1 (see Eq. (12)). Such a scenario may be reasonable if the geometric configuration of the shear walls is known a-priori and only the building imperfections are taken into account.

The results of Monte Carlo simulations are presented in the columns 3-4 of the Table 1. The probability of failure (overloading of a single wall) of a two-story building in a single year period is 0.1% for the plate model, but 1.2% for the beam model. The most vulnerable wall is W1 on the ground floor. Table 2 shows shear forces (maximum, minimum, mean value) in the individual walls acting in the y direction.

Let's now investigate the situation when the walls contain openings such as doors or windows. To simulate this situation, a set of discrete multipliers of 0.3, 0.6, 0.8 and 1.0 was introduced. The multipliers represent the reduction in stiffness due to the presence of openings. A factor of 1.0 represents a wall without any openings; a factor of 0.3 represents a wall with large openings. A uniform distribution was used to simulate an equal probability of occurrence for each opening size. The columns 5-6 of Table 1 show the corresponding probabilities for the two-story model. Fig. 5 shows the distribution of the wall stiffness for the fixed geometry and Fig. 5b shows the distribution of the wall stiffness affected by both the presence of openings (uniform distribution) and the uncertainty in stiffness itself (normal distribution). The bi-modal shape of the histogram in Fig. 5b indicates the stepwise effect of the stiffness multipliers. The first mode corresponds to the multiplier of 0.3 and the second one represents the joint effect of the remaining stiffness multipliers. Since the next multiplier starts at 0.6 and all other multipliers are equally spaced we obtained a distinct bi-modal distribution. The bi-modal (or even multi-modal) shape is expected for a superposition of a normally distributed random variable and a variable that attains several discrete values of equal probability.

From the data in Tables 1 and 2, it is evident that the plate model exhibits a higher stiffness because of its ability to capture torsional deformation modes and the contribution of the cross-walls to the building's overall stiffness. The beam model is two-dimensional and cannot capture the cross-wall contributions to the building's lateral stiffness.

The last two columns in Table 1 illustrate the effect of openings on the resistance of an LFB to

Table 1 Probability of failure (overloading) of the individual walls. Two-story model, 100000 simulations. Only walls oriented in y direction are listed. Failure defined as loss of wall stiffness – see Fig. 3

Story	Wall	Plate model	Beam model	Plate model	Beam model
		wall type is fixed		wall type varies	
1	W1	0.00115	0.01191	0.07211	0.16707
1	W2	0.0009	0.00514	0.06531	0.12695
1	W3a	0.00019	0.00014	0.03249	0.02879
1	W3b	0.00026	0.00022	0.04058	0.03708
1	W3c	0.00021	0.00017	0.03166	0.02793
1	W4a	0.00012	0.00005	0.0139	0.00623
1	W4b	0.00006	0.00004	0.01507	0.00725
2	W1	0.00000	0.00002	0.00035	0.00331
2	W2	0.00001	0.00001	0.0003	0.00176
2	W3a	0.00000	0.00000	0.00014	0.00013
2	W3b	0.00000	0.00000	0.00017	0.00014
2	W3c	0.00000	0.00000	0.00008	0.00005
2	W4a	0.00000	0.00000	0.00008	0.00008
2	W4b	0.00000	0.00000	0.00002	0.00009

Table 2 Shear forces in walls for fixed wall type [kN]. Two-story model, 100000 simulations. Only walls oriented in y direction are listed

Story	Wall	Plate model			Beam model		
		Min	Max	Mean	Min	Max	Mean
1	W1	2.41493	10.2179	5.50022	1.66943	13.3926	6.483
1	W2	1.08312	8.32357	4.36965	1.32171	11.0938	4.90572
1	W3a	1.49775	6.92939	3.86425	1.47505	6.87739	3.75538
1	W3b	0.25656	1.62157	0.759755	0.245031	1.62618	0.738408
1	W3c	1.4373	7.12396	3.86537	1.39142	6.96625	3.75643
1	W4a	1.71785	8.08469	4.17809	0.299147	9.00073	3.48047
1	W4b	1.27062	6.82792	3.49258	0.233306	7.39134	2.91051
2	W1	1.0909	5.86463	2.85618	-0.057814	8.06409	3.36593
2	W2	0.815268	4.58938	2.2691	0.632613	5.71666	2.54643
2	W3a	0.677066	4.12335	2.0074	0.633634	4.32369	1.95078
2	W3b	0.143426	0.815176	0.395019	0.132955	0.857748	0.383915
2	W3c	0.685679	4.08257	2.00987	0.64078	4.12191	1.95313
2	W4a	0.774931	4.74467	2.16763	-0.424649	5.385	1.80677
2	W4b	0.531117	4.11043	1.81609	-0.353825	5.25958	1.51433

lateral loads when the location and size of the openings are unknown. The presence of openings significantly increased the failure probability expressed at various displacement levels. Again, the contribution of transverse walls in the plate model makes the system stiffer.

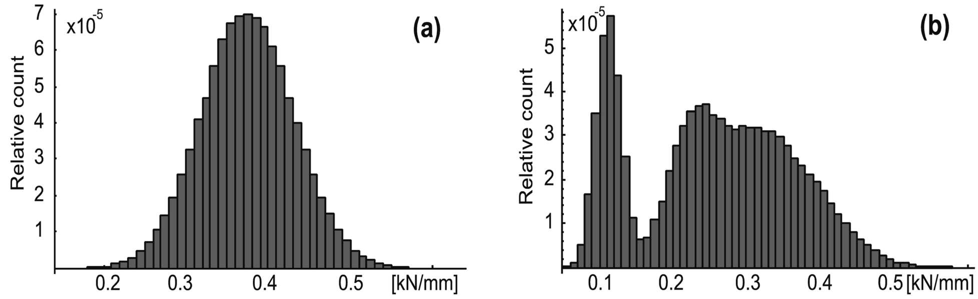

Fig. 5 Example of the distribution of the wall stiffness when the wall geometry is held fixed (a) and vary (b) (for wall W1)

4. Limitations of the models

The analytical models discussed above can only capture the global failure modes expressed as the lateral (shear deformations) or forces in individual walls. Local failure modes cannot be investigated due to the global nature of the models. Currently, the models are massless and limited to static analysis. A dynamic analysis will require reformulating the models and solution strategy. The beam model does not capture the contribution of the transverse walls to the building's stiffness and therefore overestimates the deformation of the building. The plate model captures the two dimensional behavior of the system and the contribution of all shear walls to the building's resistance to lateral loads. The bending stiffness of walls and any diaphragm distortion (such as racking) are not accounted for in either model. While the models cannot address the local failure modes of LFBs, they can be used as a tool to simulate various design scenarios and irregular building shapes to refine current prescriptive codes governing bracing in residential construction.

5. Conclusions

Simple analytical models can be used to evaluate the probability of failure of LFBs under lateral loads. In this case, the drift in a single wall was used as a failure criterion but the models permit us to define other variables as limiting factors for failure decision. These can include global building displacement, ultimate forces in walls, diaphragm rotation or a combination thereof. The models are efficient and capture the global behavior of the LFB. The two-dimensional, rigid-plate model can be used to evaluate various geometries and both models can serve as tools in the development of prescriptive or performance-based design codes where the system effect is, at least partially, accounted for. Both models can be used in estimating reaction forces in shear walls. The plate model can be used in estimating shear forces in non-rectangular buildings with or without internal walls designated as braced lines. This can be particularly valuable in refining standards governing the design of bracing systems in low-rise, light-frame buildings.

Acknowledgement

This work was partially supported by USDA grant 04-JV-11111130-106 and the Bernard and Henrietta Hankin Chair in Residential Building Construction. The support of the grant GA CR 103/03/P080 is gratefully acknowledged.

Nomenclature

$\Delta_{s,i}$, ($\delta x_{s,i}$, $\delta y_{s,i}$)	deformations of the walls in the directions y for the beam model and x and y for the plate model in the point i at the level s
$k_{x,s,i}(\delta x_{s,i})$, $k_{y,s,i}(\delta y_{s,i})$	stiffnesses of the walls in the directions x and y in the point i at the level s
$m_{x,s}$, $m_{y,s}$	number of walls in the direction x , y at the level s
N	number of floors of the building
$F_{x,s}$, $F_{y,s}$	the external forces in directions x and y
$\rho_{x,s}$, $\rho_{y,s}$	x and y coordinates of the point where the forces $F_{x,s}$ and $F_{y,s}$ are acting
ξ_σ, η_σ, ϕ_σ	components of the rigid body translations and rotation of the diaphragm s
λ_s, γ_s	components of the rigid body translations and rotation of the rigid beam
v	wind speed
ρ_a	air density
A	exposed area
c	pressure coefficient
$P_v(v)$, $p_v(v)$	cumulative density function, distribution function of Reverse Weibull distribution
α, θ, ζ	coefficients of the Reverse Weibull distribution
χ_1, χ_2	random variables

References

Adams, B.J., Womble, J.A., Mio, M.Z., Turner, J.B., Mehta, K.C. and Ghosh, S. (2004), *Collection of satellite-referenced building damage information in the aftermath of Hurricane Charley*, Natural Hazard Research and Applications Information Center, Boulder, Colorado, U.S.A.

American Society of Civil Engineers (2005), *Minimum Design Loads for Buildings and Other Structures*, ASCE/ SEI 7-05, ASCE New York, ISBN 0784408092.

Collins, M., Kasal, B., Paevere, P.J. and Foliente, G.C. (2005b), "Three-dimensional model of light-frame wood buildings, II: Experimental investigation and validation of analytical model", *J. Struct. Eng.,* **131**, 684-692.

Collins, M., Kasal, B., Paevere, P.J. and Foliente, G.C.(2005a), "Three-dimensional model of light-frame wood buildings, I: Model formulation", *J. Struct. Eng.,* **131**, 676-683.

Cook, R.A. and Soltani, M. (eds) (1994), *Hurricanes of 1992*, American Society of Civil Engineers, New York, NY.

Corotis, R.B. and Dougherty, A.M. (2004), "Reliable design loads for natural phenomena: Illustration with wind speeds", *Natural Hazard Review,* **5**, 40-47.

Extreme Wind Speed Data Sets: Daily Maxima, Database provided by NIST, http://www.itl.nist.gov/div898/ winds/daily.htm.

Foliente, G.F., Kasal, B., Paevere, P. and Collins, M. (2000), "Whole building testing and modeling for improved design of light-frame buildings", *Proc. ASCE Structures Congress*, Philadelphia. (M. Elgaaly, ed.), ASCE CD-ROM.

Grigoriu, M. (2006), *Probabilistic Models for Directionless Wind Speeds in Hurricanes*, NIST GCR 06-906, http://www.itl.nist.gov/div898/winds/pdf_files/GCR06-906.pdf.

Hanzlík, P., Diniz, S., Grazini, A., Grigoriu, M. and Simiu, E. (2005), "Building orientation and wind effects estimation", *J. Eng. Mech*., **131**, 254-258.

IRC (2006), *International Residential Code® For One- and Two-Family Dwellings*, International Code Council, ICC Whittier, CA.

Kasal, B. and Crandell, J. (2007), *Part 1: Basic Components for Code Compliant Bracing*, Builders Brief: BB0807, Pennsylvania Housing Research Center, State College, Pennsylvania, U.S.A.

Kasal, B., Collins, M., Foliente, G. and Paevere, P. (1999), "A hybrid deterministic and stochastic approach to inelastic modeling of light-frame buildings", *Proc. from 1st Int. RILEM Symposium on Timber Engineering*, L. Boström (ed.), RILEM publications, Stockholm, Sweden, ISBN 2-912143-10-1, 61-70.

Kasal, B., Collins, M., Paevere, P.J. and Foliente, G.C. (2004), "Design models of light-frame wood buildings under lateral loads", *J. Struct. Eng.,* **130**, 1263-1271.

Memari, A., Kasal, B., Adams, A. and Manbeck, A. (2008), "Comparison of in-plane lateral load resistance of interior steel stud and wood stud light-frame walls", *Proc. ASCE Structures Conf.*, Vancouver, British Columbia, Canada.

Paevere, P.J., Foliente, C. and Kasal, B. (2003), "Load-sharing and redistribution in a one-story woodframe building", *J. Struct. Eng.*, **129**, 1151-1286.

Pinelli, J.P., Simiu, E., Gurley, K., Subramanian, C., Zhang, L., Cope, A., Filliben, J.J. and Hamid, S. (2004), "Hurricane damage prediction model for residential structures", *J. Struct. Eng.,* **130**, 1685-1691.

Rosowsky, D.V. and Cheng, N. (1999a), "Reliability of light-frame roofs in high-wind regions, I: Wind loads", *J. Struct. Eng.,* **125**, 725-733.

Rosowsky, D.V. and Cheng, N. (1999b), "Reliability of light-frame roofs in high-wind regions, II: Reliability analysis", *J. Struct. Eng.,* **125**, 734-739.

Sadek, F., Diniz, S., Kasperski, M., Gioeffre, M. and Simiu, E. (2004), "Sampling errors in the estimation of peak wind-induced internal forces in low rise structures", *J. Eng. Mech.*, **130**, 235-239.

Sadek, F. and Simiu, E. (2002), "Peak non-Gaussian wind effects for database-assisted low-rise building design", *J. Eng. Mech.,* **128**, 530-539.

Simiu, E. and Scanlan, R. (1996), *Wind effects on structures*, 3rd edition, J. Wiley & Sons, New York.

Smith, I. and Kasal, B. (2004), "Monitoring of environmental loads on timber buildings", *Structures 2003-Building On The Past: Securing The Future, G. E. Blandford (ed.), Proc. ASCE Structures Congress*, Nashville, TN. ASCE New York, NY. 1-10, 0-7844-0700-2.

Whalen, T. M., Simiu, E., Harris, G., Lin, J. and Surry, D. (1998b), *Aerodynamic databases and electronic standards for wind loads: A pilot application*. NIST SP 931; August 1998, U.S./Japan Natural Resources Development Program (UJNR), *Wind and Seismic Effects. Joint Meeting of the U.S./Japan Cooperative Program in Natural Resources Panel on Wind and Seismic Effects*, 30th. May 12-15, 1998, Gaithersburg, MD, Raufaste, N. J., Jr., (eds), 506-514.

Whalen, T., Simiu, E., Harris, G., Lin, J. and Surry, D. (1998a), "The use of aerodynamic databases for the effective estimation of wind effects in main wind-force resisting systems: application to low buildings", *J. Wind Eng. Ind. Aerod.,* **77&78**, 685-693.

JH